COMPARISON OF BURIED CONTACT- AND SCREEN PRINTED 100% UMG SOLAR CELLS RESULTING IN 16.2% EFFICIENCY

Stefan Braun, Bernd Raabe, Dietmar Kohler, Sven Seren, Giso Hahn
University of Konstanz, Department of Physics, P.O. Box X916, 78457 Konstanz, Germany
Author for correspondence: stefan.braun@uni-konstanz.de, Tel.: +49 7531 882082, Fax: +49 7531 883895

ABSTRACT: In this paper we analyzed multicrystalline upgraded metallurgical grade silicon (UMG) wafer material. This was done by comparison of two different solar cell processes with a detailed analysis of the process steps. The screen printing process is a well known and widespread industrial standard solar cell process, which offers good results and serves as a reference process. Due to an effective bulk passivation with hydrogen the screen printed solar cells have a high internal quantum efficiency (IQE) in the long wavelength regime. The buried contact solar cell process is a high efficiency cell process which offers due to a selective emitter design and low shading losses excellent results on Cz wafer material. The selective emitter structure offers a high IQE in the blue response. Additional characterization of the bulk by spatially resolved bulk lifetime measurement, internal quantum efficiency and reflection measurements for both solar cell processes was performed. Screen printed solar cells with efficiencies up to 16.2% and buried contact solar cells with efficiencies up to 15.5% were produced.
Keywords: Metallurgical-Grade, Buried Contacts, Screen Printing

1 INTRODUCTION

The use of new wafer material for the production of solar cells offers a great possibility of cost reduction. Usually a more cost effective material leads to less efficient solar cells. In the past it was shown that UMG material can be used to produce screen printed solar cells with efficiencies up to 16% on 125 mm x 125 mm wafer material [1]. Furthermore up to 18.5% efficiency was reached on UMG material on 20 mm x 20 mm wafers [2].

We analyzed UMG multicrystalline wafer material for two different processes. A high efficiency buried contact solar cell process was contrasted with a screen printing solar cell process. For the experiment neighboring wafers from the same brick were used for comparison.

Both processes offer different opportunities for the material. The first question was if the UMG material can withstand the different high temperature steps during solar cell production. The second question was if the screen printing process which is easier to handle because of less production steps could reach similarly high efficiencies as for the buried contact process.

For the electroless metallization process of the buried contact solar cells, it was possible to integrate a nickel sintering step to the process, which is expected to improve the contact resistance and the adhesion of the metallization.

Afterwards the reflection, spectral response and the IV parameters were measured. Spatially resolved lifetime and LBIC maps indicate the differences of both processes.

2 THE BURIED CONTACT CELL PROCESS

The high efficiency solar cell process was implemented via a buried contact solar cell process on 125 mm x 125 mm, 190 µm thick multicrystalline UMG silicon wafers which were isotextured. The process sequence is shown in figure 1 on the left side. A buried contact solar cell has a selective emitter structure and contact grooves for the front site metallization. The grooves were formed by dicing. As antireflection coating low pressure chemical vapor deposition (LPCVD) silicon nitride was used. The metallization was obtained by electroless nickel and copper plating.

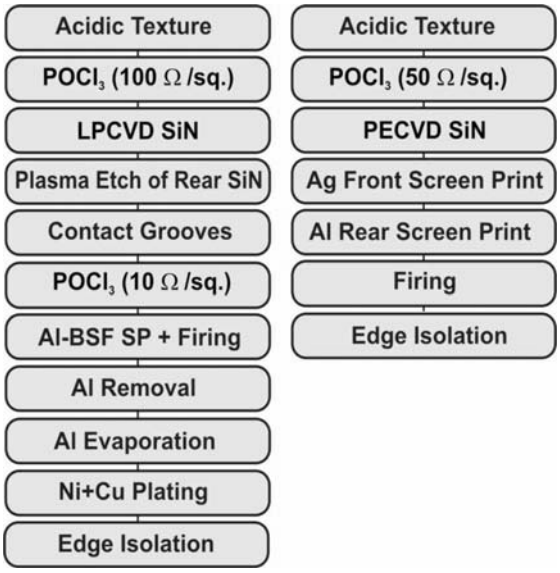

Figure 1: Process sequences of the different solar cell types. On the left the buried contact solar cell process and on the right the screen printing solar cell process is shown.

The aluminum back surface field was formed by a screen printed aluminum layer. Afterwards the solar cells were fired in a belt furnace. The residues of the aluminum layer were etched back in hydrochloric acid. Aluminum was evaporated on the back side of the cell to create an approximately 2 µm thick layer. The nickel layer was deposited on the aluminum layer. Before plating a short dip in hydrofluoric acid was performed to remove the oxide layer formed on the silicon and aluminum surface. A thin seed layer was deposited on the front and back site of the cell at 50°C in a nickel containing solution for 3 minutes. This seed layer was thickened by an additional nickel layer, the so called base layer. To form the base layer a different solution was

heated up to 80°C and the wafers were plated for additional 5 minutes. These two layers serve as electrical contact and as a diffusion barrier for the copper layer. The copper layer provides a good conductivity and a low series resistance.

3 NICKEL SINTERING

The deposition of the nickel seed layer offered the possibility of sintering the cells afterwards to create a nickel silicide with an improved contact resistance and adhesion compared to a non sintered cell. The nickel silicide NiSi starts to form at temperatures between 300°C and 700°C and has a low contact resistance which is comparable to Ti Si_2 [3].

A thin 100 – 200 nm thick nickel seed layer was deposited by an electroless plating step at 50°C for 3 minutes. A group of solar cells was not sintered. A tube furnace was heated up to 450°C and the cells were sintered for 120 minutes in a nitrogen atmosphere to create a nickel silicide. Afterwards the base layer was deposited on the sintered seed layer at 80°C for 5 minutes.

Experiments within an atomic hydrogen atmosphere during the sintering were executed. Therefore a plasma generator was mounted at the furnace. At last copper was deposited on the thickened layer for 3 hours at 42°C.

4 THE SCREEN PRINTING CELL PROCESS

The screen printing process is a well established process for solar cell production. Figure 1 on the right hand shows the process sequence. Starting with a 125 mm x 125 mm isotextured 190 µm thick multicrystalline UMG silicon wafer and 50 Ohm/sq emitter diffusion the PECVD silicon nitride is deposited on the surface of the wafer. The front side metallization consists of a silver paste and the backside consists of an aluminum paste, both are printed with a screen printer. After a firing step in a belt furnace the cell has to be edge isolated, this was done with a dicing saw.

5 CELL RESULTS

The solar cells showed good results using the screen printing process. The best result was 16.2% efficiency with a fillfactor of 79.7% out of two cells. The high efficiency buried contact process was not as efficient as the screen printing process. Cells reached maximum efficiency of 15.5% and a fillfactor of 75.8% could be produced without sintering. Further IV data is shown in table I.

A more detailed analysis of the cells revealed why the high efficiency process was not as effective as estimated. The additional nickel sintering step showed no impact on the cell performance. The sintering process in hydrogen plasma was also inefficient. The fillfactors of the solar cells were low because of a high contact resistance.

Table I: IV data of the best screen printed (SP) and the buried contact (BC) solar cell.

	Shading [%]	**J_{SC} [mAcm²]**	**V_{OC} [mV]**	**FF [%]**	**Eta [%]**
BC	5.1	33.3	613.2	75.8	15.5
SP	8.3	32.6	627.5	79.4	16.2

During the electroless nickel plating process an oxidation of the metallization layer may occur which could have caused an oxide stack between the two nickel layers which could explain the high contact resistance.

6 ANALYSIS OF THE SOLAR CELLS

Reflection measurements revealed that the reflection of the buried contact cell is lower in the short wavelength regime. In the long wavelength regime the reflections are comparable.

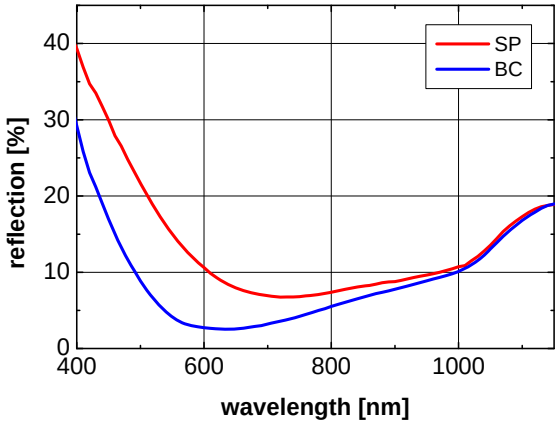

Figure 2: Reflection of a buried contact cell (BC) compared to a screen printed cells (SP). Measured area without busbar shading.

A result of the different reflection curves shown in figure 2 is shading, which is 5.1% for the BC solar cell due to thinner fingers and 8.3% for the SP solar cell including busbars. The thickness of the silicon nitride is indicated by the two minima of the reflectance graphs, one can see clearly that the BC solar cell has a thinner silicon nitride coating.

The minimum of reflectance for the buried contact solar cell is located at 640 nm. The minimum of the screen printed cell is at 720 nm. The minimum of reflectance for both graphs is lower than the shading values because the measurement was done at a busbar free area of the solar cells.

The internal quantum efficiency is plotted in figure 3. In the short wavelength regime the internal quantum efficiency for the buried contact cells is higher compared to the screen printed cells. This can be explained due to less recombination of the charge carriers in the dead layer.

However, the screen printed solar cell has advantages in the long wavelength regime. This indicates that the bulk passivation of the screen printed solar cell is better than the passivation of the buried contact cell because the back surface passivation of both cell types is the same.

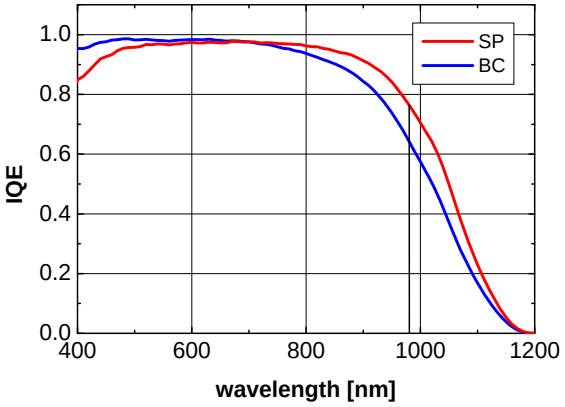

Figure 3: Internal quantum efficiency of the buried contact cell (BC) compared to the screen printed cell (SP).

Due to a higher hydrogenation level due to the PECVD silicon nitride the screen printed solar cells profit from a higher bulk lifetime. To quantify the beneficial effects of the hydrogenation of the bulk defects, the bulk was characterized in detail.

7 LBIC MEASUREMENTS AND CHARACTERISATION OF THE BULK LIFETIME

For a detailed analysis of the bulk spatially resolved lifetime measurements were performed using Microwave Photo Conductance Decay (µ-PCD) see also [4].

For an optimal process monitoring the lifetime samples were performed throughout the whole production process. After the final production step the metallization was etched back in hydrofluoric acid solution and afterwards rinsed in DI H_2O.

The silicon nitride was removed in diluted hydrofluoric acid and rinsed in DI H_2O. To ensure that the aluminum back surface field is not present in the bulk anymore the wafer was etched back in CP6 solution. For the µ-PCD measurement the wafers were cleaned in a piranha etching solution followed by a diluted hydrofluoric dip. To define the spatial resolved bulk lifetime,µ-PCD method was used. The surface was passivated with iodine-ethanol-solution for the lifetime measurements.

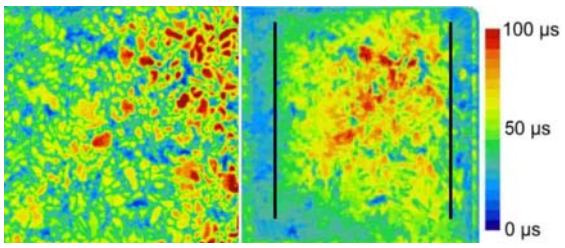

Figure 4: Lifetime maps for the BC cell (left) and the SP cell (right). The surface of the edge region (indicated) of the SP cell is not well passivated.

The lifetime maps are shown in figure 4, on the right side the screen printed (SP) and on the left side the buried contact (BC) solar cell is represented. The surface of the edge regions of the screen printed solar cell is not well passivated, most probably due to problems with the iodine/ethanol solution. On the left side one can see regions of high and low lifetime separated by grain boundaries.

The grain boundaries on the right side are better passivated and even large dislocation clusters seem to be passivated well. The multicrystalline structure of the BC solar cell on the other hand contains dislocations which are not passivated well. The average bulk lifetime of the BC solar cell is 50 µs. The bulk lifetime of the screen printed solar cell was measured with 48 µs which is supposed not to be a realistic value. One can see on the left and the right edges (marked area in figure 4) of the SP solar cell that the lifetime decreased. The areas at the edge of the wafer were probably measured too low because of passivation problems with the iodine/ethanol solution. In figure 5 spatially resolved LBIC maps for the wavelength 980 nm are presented.

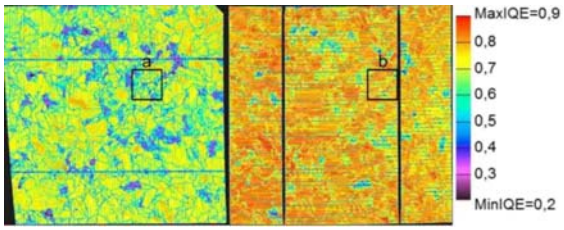

Figure 5: Spatially resolved LBIC maps (980 nm) of the BC cell (left) and the SP cell (right).

The average IQE of the BC solar cell is 0.62 and the IQE of the SP solar cell is 0.69.

For a more detailed analysis high resolved LBIC maps were made of the marked regions (a) and (b) in figure 5 and are presented in figure 6.

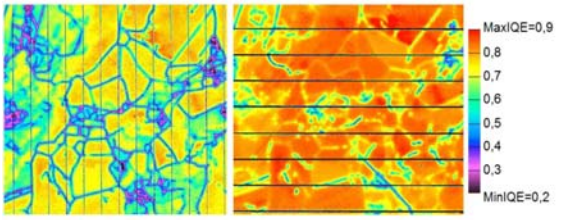

Figure 6: High resolution LBIC maps (980 nm) of the BC cell (left) and the SP cell (right) in figure 4. The area of the cells is marked in Figure 4 with (a) and (b).

In these pictures the passivation of the grain boundaries is obvious. The IQE of the grain boundaries of the buried contact solar cell is in a range in between 0.5 and 0.6 in contrast to the grain boundaries of the screen printed solar cell which exhibit an IQE in between 0.6 and 0.75. Even large dislocation clusters were passivated well as a result of the differences in the silicon nitride and the high temperature steps during the production of the cells. The lifetime maps for each production step can be found in [4].

During the LPCVD silicon nitride deposition of the buried contact cell the hydrogen contained in the nitride diffuses out of the bulk because of the high temperature during the deposition but this hydrogen is needed for the bulk passivation. This phenomenon causes the lower IQE of the BC cell in the long wavelength regime. During the

PECVD silicon nitride deposition the hydrogen stays in the silicon nitride layer because of lower temperature. This hydrogen is capable for passivating the bulk during the firing step of the front and rear side metallization.

8 CONCLUSION

An electroless nickel and copper plating sequence was used for front- and rear side metallization of the buried contact solar cells. Attempts to sinter the solar cells in a furnace with nitrogen or hydrogen atmosphere were undertaken and showed no significant enhancement in the cell performance because of high contact resistance.

The used 100% UMG wafer material is able to withstand the high temperature steps of a buried contact cell process which is not natural for multicrystalline silicon [5]. Screen printed solar cells produced on the same wafer material using neighboring wafers showed even better performance. Due to a higher IQE in the long wavelength regime the screen printed solar cells reached efficiencies up to 16.2%, though the shading was nearly twice as high as the reduced shading of the buried contact solar cells. Due to the PECVD silicon nitride antireflection coating which provides a high amount of hydrogen a higher passivation level than with the LPCVD silicon nitride was reached in the bulk. This was demonstrated by LBIC measurement. The LBIC measurement showed the difference in bulk passivation of the cell types. The mean IQE of the screen printed solar cell was 0.69 compared to 0.62 of the buried contact solar cell.

The buried contact solar cell shows less passivated grain boundaries and dislocation clusters as the screen printed solar cell. This was also indicated by the spectral response measurement.

9 OUTLOOK

Combining the two cell concepts would create a high efficiency solar cell with a high IQE in the blue response and in the short wavelength regime. This could only be done with an additional hydrogenation step of the buried contact solar cell or a new cell concept without using LPCVD and a second emitter diffusion in a furnace after silicon nitride deposition.

If a combined sintering and hydrogenation step will be effective on that UMG wafer material the cell would profit due to a reduced contact resistance and a sufficient bulk hydrogenation.

10 ACKNOWLEDGEMENTS

The financial support from the BMU project 0325079 is gratefully acknowledged in particular for the sample characterization.

The authors would like to thank S. Ohl, B. Rettenmaier, L. Rothengaß, A. Müller, J. Ruck and J. Ruck for their steady support during cell process.

11 REFERENCES

[1] K. Peter, R. Kopecek, T. Pernau, E. Enebakk, K. Friestad, R. Tronstad, C. Dethloff, *"Analyses of multicrystalline solar cells from solar grade silicon feedstook"*, Proc. 31st IEEE PVSC, Lake Buena Vista, 2005, p. 927

[2] M. Kaes, G. Hahn, K. Peter, E. Enebakk, *"Over 18% efficient mc-Si solar cells from 100% solar grade silicon feestock from a metallurgical process route"*,Proc. 4th WCPEC Waikoloa, 2006, p. 873

[3] D. S. Kim, E J. Lee, J. Kim, S. H. Lee, *"Low-cost contact formation of high-efficiency crystalline silicon solar cells by plating"*,Journal of the Korean Physical Society, Vol. 46, No. 5, May 2005, p. 1208

[4] D. Kohler, B. Raabe, S. Braun, S. Seren, G. Hahn, *"Upgraded Metallurgical-Grade Silicon Solar Cells: A Detailed Analysis"*, Proc. 24th EU-PVSEC, Hamburg, 2009

[5] B. Raabe, K. Peter, E. Enabakk, G. Hahn, *"Minority carrier lifetime monitoring in a buried contact solar cell process using mc-Si"*, Proc. 23th EU-PVSEC, Valencia 2008, p. 1564